Applied Catalysis B: Environmental 90 (2009) 426–435

Contents lists available at ScienceDirect

Applied Catalysis B: Environmental

journal homepage: www.elsevier.com/locate/apcatb

Synthesis of DME from syngas on the bifunctional Cu–ZnO–Al_2O_3/Zr-modified ferrierite: Effect of Zr content

Jong Wook Bae, Suk-Hwan Kang, Yun-Jo Lee, Ki-Won Jun *

Petroleum Displacement Technology Research Center, Korea Research Institute of Chemical Technology (KRICT), P.O. BOX 107, Yuseong, Daejeon, 305-600, Republic of Korea

ARTICLE INFO

Article history:
Received 16 January 2009
Received in revised form 31 March 2009
Accepted 2 April 2009
Available online 9 April 2009

Keywords:
Syngas
Dimethyl ether
Ferrierite
Zirconium
Cu–ZnO–Al_2O_3
Bifunctional

ABSTRACT

The catalytic activity on the coprecipitated Cu–ZnO–Al_2O_3/Zr-ferrierite (CZA–ZrFER) with different Zr content from 0 to 5 wt.% was investigated for the direct synthesis of dimethylether (DME) from H_2-deficient and biomass-derived model syngas (H_2/CO molar ratio = 0.93). The catalytic functionalities, such as CO conversion and DME selectivity, showed their maxima on the bifunctional catalyst with 3 wt.% Zr-modified ferrierite. Detailed characterization studies were conducted on the catalysts to measure their properties such as surface area, acidity by temperature-programmed desorption of ammonia (NH_3-TPD), reducibility of Cu oxide by temperature-programmed reduction (TPR), copper surface area measurements by N_2O titration method, electronic states of copper by IR analysis and particle size measurement by XRD and TEM analysis. The number of acid sites measured by NH_3-TPD on the bifunctional catalysts decreased monotonously with the increase of Zr content, meanwhile, the acidic strength is found to be minimal on the catalyst showing best performance. The reducibility of copper oxide and the surface area of metallic copper also exhibited their maximum values at the same Zr composition indicating that these are responsible for the optimum functionality of the bifunctional CZA–ZrFER catalyst. The role of easily reducible copper species with small particle size and the suppressed strong acidic sites is also emphasized in the consecutive reaction from syngas to DME on the bifunctional catalyst. The different behavior of intrinsic rate of the bifunctional catalysts is also well correlated with the metallic surface area of copper and the amount of acidic sites with their acidic strength.

© 2009 Elsevier B.V. All rights reserved.

1. Introduction

Dimethylether (DME) is one of the important chemicals for the production of dimethyl sulfate, methyl acetate and light olefins and it is also considered to be an environmentally benign alternative clean fuel since it is easily handled and transported by using the infrastructure of LPG transportation due to its similar physical properties [1]. In addition, as the oil resources are expected to deplete in near future. Alternative fuels such as a biomass-derived DME and methanol have been getting greater attention to minimize the emissions of global warming gases and hazardous components such as SOx, NOx and particulate matter. Furthermore, DME could be one of the possible candidates to supply hydrogen-rich fuel cell feed gas by autothermal reforming or steam reforming process [2]. The general process for the production of DME from syngas consists of the synthesis of methanol by hydrogenation of CO and/or CO_2 on Cu–ZnO-based catalysts followed by the production of DME by dehydration of MeOH on a solid acid catalyst like γ-Al_2O_3 or modified ZSM-5 zeolite [3,4]. However, a lot of emphasis has been laid on the development of a single-step process for the direct synthesis of DME in a fixed-bed or slurry reactor [5] using bifunctional catalysts that exhibit the above two functionalities. A single-step reaction (syngas to DME; STD) of biomass-derived H_2-deficient and CO_2-abundant syngas [6] has gained tremendous attention for the synthesis of DME, due to its ability to produce renewable fuel with high potential to minimize the pollutant emissions into the atmosphere and thereby to reduce global warming. Preparation of bifunctional catalysts is a challenging process and it needs special efforts to balance the two functionalities (active sites for CO hydrogenation and dehydration of methanol). There are a few methods to achieve highly active and selective bifunctional catalyst. For example, the preparation of highly dispersed fine crystallites of skeletal Cu with high surface area can be achieved by changing the preparation conditions and eventual stabilization of active Cu species by adding promoters [7,8]; modification of acidity of bifunctional catalyst by modifying ZSM-5 with Fe [9] or Mg [10] and changing the silica-to-alumina ratio of amorphous silica–alumina catalyst [11]. The modification of acidity is a key variable to enhance the DME selectivity and to suppress further

* Corresponding author. Tel.: +82 42 860 7671; fax: +82 42 860 7388.
E-mail address: kwjun@krict.re.kr (K.-W. Jun).

0926-3373/$ – see front matter © 2009 Elsevier B.V. All rights reserved.
doi:10.1016/j.apcatb.2009.04.002

dehydration of DME into undesired hydrocarbons. In our previous investigation, a superior catalytic performance was demonstrated on Zr-modified ferrierite bifunctional catalyst in terms of high CO conversion and DME selectivity compared to the ZSM-5 and Y zeolite-based bifunctional catalysts, owing to the facile reducibility of metal component and the presence of proper amount of acid sites that existed on the former [12]. The superiority of ferrierite also lies in its favorable topology facilitating easy diffusion of the reactants and products [13]. Although much work is reported on the role of acidity of the solid acid component, the importance of Zr composition in the bifunctional catalyst containing Cu–ZnO–Al_2O_3 and Zr-modified ferrierite is not investigated for the direct synthesis of DME from biomass-derived syngas.

Thus, the present investigation is focused on understanding the influence of Zr content on Zr-modified ferrierite which is introduced during the coprecipitation of Cu–ZnO–Al_2O_3 components to make a bifunctional catalyst on the CO conversion and DME selectivity to utilize biomass-derived syngas efficiently. The characterization of the bifunctional catalyst using various methods such as nitrogen adsorption, X-ray diffraction (XRD) analysis, the measurement of metallic copper surface area, temperature-programmed desorption of ammonia (NH_3-TPD), temperature-programmed reduction (TPR), X-ray photoelectron spectroscopy (XPS), Fourier-transformed infrared (FT-IR) spectroscopy and transmission electron microscope (TEM) are utilized to study the effect of Zr content on the bifunctional Cu–ZnO–Al_2O_3/Zr-modified ferrierite catalyst for STD reaction.

2. Experimental

2.1. Preparation of bifunctional catalysts

The Cu–ZnO–Al_2O_3/Zr-ferrierite bifunctional catalyst (CZA/ZrFER) consisting of 7:3 ratio of Cu–ZnO–Al_2O_3 component (denoted as CZA, active components for methanol synthesis) and Zr-ferrierite component (denoted as ZrFER, active one for DME synthesis) with different Zr content was prepared by coprecipitation method in the slurry of ZrFER. The H-ferrierite has a surface area of 364 m^2/g and a pore volume of 0.13 cm^3/g. For the bifunctional CZA/ZrFER catalyst, a metal oxide composition was 50 wt.% CuO, 40 wt.% ZnO, and 10 wt.% Al_2O_3. In order to prepare the metal oxides the metal nitrates were selected as their precursors. The weight ratio of CZA component to ZrFER was further verified by XRF analysis. The ZrFER was prepared by loading Zr precursor ($ZrCl_2O{\cdot}8H_2O$) on the ferrierite (Si/Al = 25 provided by Zeolyst) with different Zr contents from 0 to 5 wt.% by slurry impregnation method. The ZrFER was previously calcined at 400 °C for 5 h under flowing air before making a bifunctional CZA–ZrFER catalyst. The bifunctional CZA–ZrFER catalyst was prepared by coprecipitation of CZA component in the slurry of ZrFER by using the Na_2CO_3 as a precipitant at a pH of around 7 and digested at 70 °C for 3 h. The finished catalyst was dried and subsequently calcined at 350 °C for 5 h in flowing air. A more detailed preparation method was reported in our previous work [12–14]. The catalysts are denoted as CZA–ZrFER(X), where CZA stands for the Cu–ZnO–Al_2O_3 component and ZrFER for the Zr-modified ferrierite. The X in the bracket denotes the Zr content such as 0, 1, 3 and 5 wt.% based on the 100 wt.% of bare ferrierite zeolite.

2.2. Catalyst characterization

The surface area and pore volume measurements were conducted by nitrogen adsorption and desorption isotherms obtained at −196 °C using a constant-volume adsorption apparatus (Micromeritics, ASAP-2400). The pore volume was determined at a relative pressure (P/P_o) of 0.99. The calcined samples were degassed at 250 °C with a He flow for 4 h before the measurements. The pore size distribution of samples was determined by the BJH (Barett–Joyner–Halenda) model from the desorption branch of the nitrogen isotherm.

The fresh and used bifunctional CZA–ZrFER catalysts were thoroughly characterized for their structural identification and crystallinity by the powder X-ray diffraction (XRD) patterns (Rigaku diffractometer using Cu Kα radiation).

The Cu metal area was measured by N_2O surface titration method by using the home-made apparatus. Prior to the titration, the fresh and used samples with 0.5 g were reduced at 250 °C for 4 h with 5% H_2/N_2 flow, followed by purging and cooling with a He flow to 100 °C. The consumption of N_2O as well as the evolution of N_2 on the metallic Cu sites ($N_2O + 2Cu = Cu_2O + N_2$) was measured at 60 °C by a thermal conductivity detector (TCD). The surface area of metallic Cu was calculated by assuming 1.46×10^{19} Cu atoms/m^2 and a N_2O/Cu_s (Cu atom on surface) molar stoichiometry of 0.5 and the particle size of Cu was calculated with the equation of 6000/(8.92 × Cu metal surface area/Cu fraction in gram catalyst) [15].

The NH_3-TPD experiments (Micromeritics, Autochem 2920) were performed to determine the acidity of calcined and used catalysts by using GC equipped with TCD. About 0.1 g of the sample was flushed initially with a He flow at 250 °C for 2 h, cooled to 100 °C and saturated with NH_3. Purging the sample with He flow was continued until equilibrium, and then TPD was carried out from 100 to 500 °C at a heating rate of 10 °C/min and kept at that temperature for 20 min.

For the temperature-programmed reduction (TPR) carried out on the BEL-CAT instrument, the sample (0.1 g) was previously treated in He flow up to 350 °C and kept for 2 h to remove adsorbed water and other contaminants followed by cooling to 50 °C. The 5% H_2/He mixture was passed over the samples at a flow rate of 30 ml/min with a heating rate of 10 °C/min up to 450 °C. The effluent gas was passed over a molecular sieve trap to remove the generated water and then analyzed by GC equipped with TCD.

The surface electronic states of copper, aluminum and zirconium species after reaction for 18 h on stream were characterized by using the XPS (ESCALAB MK-II). During the experiments, the Al Kα monochromatized line (1486.6 eV) was adopted and the vacuum level was around 10^{-7} Pa. The used samples was previously pressed to thin pallet and the binding energy (BE) were corrected by adjusting with the reference BE of Al 2s (118.6 eV).

The diffuse reflectance infrared Fourier transform (DRIFT) spectra of adsorbed CO molecule on used catalysts after re-reduction was carried out by using Nicolet Protege 460 FT-IR spectrometer equipped with a MCT detector which was cooled with liquid nitrogen and at a spectral resolution of 2 cm^{-1}. All used catalysts were reduced in situ at 250 °C for 4 h under H_2 flow. The reduced catalyst was kept at that temperature for 1 h and cooled to 50 °C under He flow to remove H_2 on the copper surfaces. And then, CO was introduced at 50 °C for 0.5 h with a flow rate of 30 cm^3/min and the CO gas was switched with He again for 40 min to remove the gaseous CO molecules. The FT-IR spectra of adsorbed CO molecules were obtained by subtracting that of reduced catalyst.

The particle size of CZA component and its chemical composition before and after reaction for 18 h was further characterized by using the transmission electron microscopy (TEM; TECNAI G2 instrument) and TEM-EDX analysis.

2.3. Catalytic activity tests

The catalytic activity was carried out in a fixed-bed stainless-steel reactor with an inner diameter of 10.2 mm using 1.0 g of bifunctional catalysts. Prior to activity test, all CZA–ZrFER catalysts

were reduced in 5% H_2/N_2 flow at 250 °C for 4 h under atmospheric pressure. The following reaction conditions were employed during activity test; T = 250 °C; P = 4.0 MPa; space velocity (SV) = 5500 L/(kg_{cat} h) and the molar feed composition of $CO/CO_2/H_2$ = 41/21/38. Based on the earlier reports on biomass gasification [2], the mixed reactant syngas was selected as a model composition. The effluent products were analyzed by an online GC (DS6200, Donam Co.) equipped with two columns; Porapack-Q connected to a TCD for non-flammable products (CO, CO_2) and GS-Q to a flame ionization detector (FID) for flammable products such as methanol, DME and hydrocarbon byproducts. The CO conversion and product selectivity were calculated based on the total carbon balance. The average values obtained at a stable activity performance after 14–16 h on stream were considered to evaluate the differences in catalytic activity.

3. Results and discussion

3.1. The catalytic performance on CZA–ZrFER bifunctional catalysts

The STD activity on the bifunctional CZA–ZrFER catalysts with varying Zr content is shown in Table 1. In general, the following reactions occur during STD reaction.

$$\text{Methanol synthesis}: \ CO + 2H_2 \rightleftarrows CH_3OH \quad \Delta H^\circ = -90.6\,\text{kJ/mol} \tag{1}$$

$$\text{Methanol dehydration}: \ 2CH_3OH \rightleftarrows CH_3OCH_3 + H_2O \quad \Delta H^\circ = -23.4\,\text{kJ/mol} \tag{2}$$

$$\text{WGS reaction}: \ H_2O + CO \rightleftarrows H_2 + CO_2 \quad \Delta H^\circ = -41.2\,\text{kJ/mol} \tag{3}$$

$$\text{Total net reaction}: \ 3CO + 3H_2 \rightleftarrows CH_3OCH_3 + CO_2 \quad \Delta H^\circ = -245.8\,\text{kJ/mol} \tag{4}$$

As predicted from the above equation, the total net reaction (Eq. (4)) is more thermodynamically favorable compared to the others (Eqs. (1)–(3)). The main advantage of the direct synthetic route to DME is to overcome the equilibrium constraint of MeOH synthesis reaction by the in situ generation of extra hydrogen through WGS reaction (Eq. (3)) which results in higher conversion of CO. Furthermore, the hydrolysis of DME to methanol (reverse reaction of Eq. (2)) is not also overlooked on solid acid catalyst. On zeolites such as ZSM-5 and zeolite Y, the conversion of DME to methanol reaches the equilibrium at 200–275 °C depending on the acidity and Si/Al ratio [16]. The CO conversion reached a maximum value of 49.0% on CZA–ZrFER(3) from 30.4% on CZA–ZrFER(0) and decreased to 29.8% on CZA–ZrFER(5). Here again, the superiority of CZA–ZrFER(3) is apparent in terms of providing the highest DME selectivity of around 58.2%. Interestingly, the highest DME selectivity is accompanied by the highest CO conversion on these catalysts. This observation is indeed in accordance with the basic mechanism of DME synthesis from syngas where the extra hydrogen produced in the water–gas-shift reaction is responsible for higher CO conversion. All catalysts show an equilibrium selectivity of around 34% to CO_2 due to the fast reaction rate of WGS reaction [17,18] except for the CZA–ZrFER(0). The CO_2 concentration in the product also reveals that the excess CO_2 formed on these catalysts is not able to undergo hydrogenation to produce methanol or DME under the present reaction conditions (low H_2 concentration with H_2/CO molar ratio of 0.93). Since CO_2 is converted to methanol at much higher H_2/CO ratio of above 3 ($CO_2 + 3H_2 = CH_3OH + H_2O$), the amount of CO_2 consumed under the present conditions, such as low H_2/CO molar ratio and high CO_2 concentration ($CO/CO_2/H_2$ = 41/21/38 mol%) in feed stream, is trivial than the amount of CO_2 formed due to WGS reaction. The Zr-modified ferrierite containing bifunctional property also shows a low activity for byproduct formation. Since the direct DME synthesis from syngas is a kind of a consecutive reaction, the partial pressure of previously formed methanol could be the crucial factor to enhance the DME selectivity due to the lowest activation barrier for the pathway of two contiguous methanol molecules adsorption compared to that of methoxy formation from one methanol adsorption [19]. In general, ferrierite zeolite has an orthorhombic framework containing one-dimensional channels of 10-membered rings and one-dimensional channels of 8-membered rings which are perpendicularly intersected. This topology is helpful in the easy diffusion of the reactants and products as reported by us earlier [13] and proper modification with Zr may further enhance the catalytic activity by controlling the copper dispersion and acidity of ferrierite. Therefore, high selectivity to DME on CZA–ZrFER(3) may be attributed to the high concentration of methanol formed and its high dehydration activity on the acidic sites, properly controlled by the deposition of Cu–ZnO–Al_2O_3 components on Zr-modified ferrierite surface. The reasons for the superior performance of CZA–ZrFER(3) have been carefully examined with the help of several characterization techniques and the results are given in Sections 3.2 and 3.3.

Table 1
Conversion and product distribution on CZA–ZrFER bifunctional catalysts.

Notation[a]	CO conversion (mol%)	Product distribution (mol%)[b]			
		CH_3OH	DME	CO_2	Byproducts
CZA–ZrFER(0)	30.4	42.8	28.7	27.9	0.6
CZA–ZrFER(1)	35.3	22.1	40.8	36.7	0.4
CZA–ZrFER(3)	49.0	7.8	58.2	33.7	0.3
CZA–ZrFER(5)	29.8	34.0	34.0	31.6	0.4

[a] The notation of CZA–ZrFER(x) catalysts stands for the Cu–ZnO–Al_2O_3 on Zr-modified ZSM5 (Si/Al = 25) with (x) weight percentage of zirconium in the range of 0–5.
[b] The CO conversion and selectivity are the averaged values obtained in the range of 14–16 h on stream and the byproducts mainly include CH_4 and higher hydrocarbons.

3.2. Textural and surface properties of CZA–ZrFER bifunctional catalysts

The pore size distribution of CZA–ZrFER catalysts are displayed in Fig. 1 and their physical properties are summarized in Table 2. All bifunctional CZA–ZrFER catalysts show a bimodal pore size distribution with mesopores of size around 30 nm possibly attributed to the inter-grain structures of CZA component and those of around 4 nm attributed to the intrinsic structure of bare ferrierite zeolite. It implies that CZA component is well dispersed on the outer surface of Zr-modified ferrierite. Interestingly, the volume of pores with size of around 4 nm on the samples (inset in Fig. 1) monotonously decreases up to 3 wt.% Zr addition on ferrierite and it again increases at 5 wt.% Zr on ferrierite. This suggests that the Zr component is homogeneously distributed at the inner pore of ferrierite up to 3 wt.%. However, its distribution is not homogeneous at high Zr content (5 wt.%) and it predominantly exists on the outer surface of ferrierite with a large particle size. The surface area of CZA–ZrFER(0) is 134.0 m^2/g due to the presence of mesopores of around 3.9 nm and it decreased to 120.8 m^2/g on CZA–ZrFER(3). This decrease of surface area from 364 m^2/g of H-ferrierite is attributed to the CZA component deposition and Zr modification during catalyst preparation. The variation of average

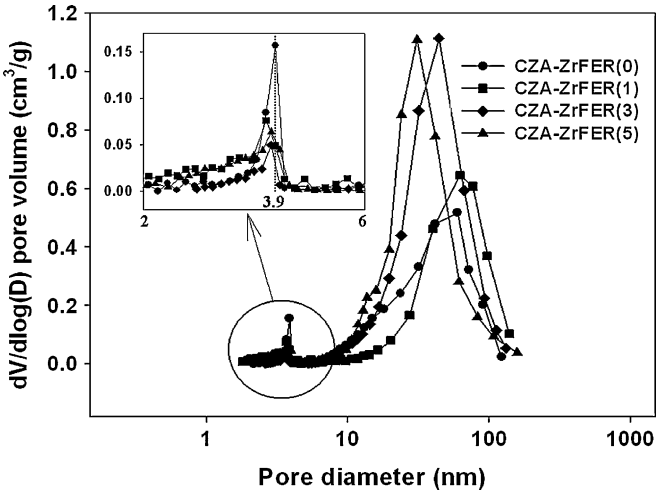

Fig. 1. Pore size distribution of the bifunctional CZA–ZrFER catalysts.

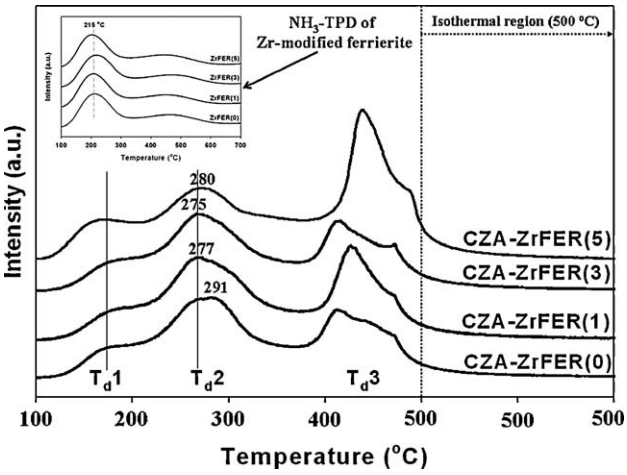

Fig. 2. NH_3-TPD profiles of the fresh bifunctional CZA–ZrFER catalysts.

Table 2
Textural properties of CZA–ZrFER bifunctional catalysts.

Notation	Surface area (m^2/g)	Pore volume (cm^3/g)	Average pore diameter (nm)
CZA–ZrFER(0)	134.0	0.33	26.1
CZA–ZrFER(1)	124.0	0.35	33.1
CZA–ZrFER(3)	120.8	0.56	32.2
CZA–ZrFER(5)	130.9	0.53	26.0

The H-ferrierite has a surface area of 364 m^2/g and pore volume of 0.13 cm^3/g.

pore diameter reveals a reverse trend to that of surface area and the smallest average pore diameter of around 26 nm is observed on CZA–ZrFER(5). The large pore volume of 0.56 cm^3/g, and moderate average pore diameter and surface area of 32.2 nm and 120.8 m^2/g respectively were observed on CZA–ZrFER(3). To obtain high catalytic activity, the larger values of those properties are beneficial by facile mass-transfer of reactants and products with the additional benefit of high concentration of active site formation. With those textural properties of CZA–ZrFER catalysts, the acidity and reducibility of copper oxides are crucial factors to get a high catalytic activity on bifunctional catalysts [8–13].

The NH_3-TPD profiles and the number of acid sites of CZA–ZrFER catalysts are summarized in Fig. 2 and Table 3, respectively. The results of NH_3-TPD reveal three different peaks, in the regions of 140–340 °C (T_d1), 340–350 °C (T_d2) and 350–550 °C (T_d3). According to the reports by Jin et al. [20], the three distinctive desorption peaks of ammonia which is characterized by TCD was assigned to different acidic sites on bifunctional catalysts. The peak T_d1 corresponds to the acid sites contributed by the zeolite matrix alone and the second peak of T_d2 is attributed to the catalyst species present on the surface of the bifunctional catalyst. However, the T_d3 peak on our samples is attributed to the amount of H_2O evolution from CZA oxide component and framework of ferrierite zeolite which is conformed by additional analysis of mass spectroscopy. The Zr-modified ferrierite with different Zr loadings (before the addition of CZA components) were also characterized by NH_3-TPD (inset in Fig. 2). The number of weak acidic sites show a trivial change but desorption temperature is shifted to lower temperature around 215 °C with increasing the Zr content. The T_d1 and T_d2 which are assigned to the active sites for methanol dehydration [7,10–14] are also shifted to lower temperatures. The desorption temperature (T_{max})of T_d2 is found to be minimum on CZA–ZrFER(3) at around 275 °C and maximum on CZA–ZrFER(0) at around 291 °C. The strong acidic sites of T_d2 are possibly responsible for the byproducts or coke formation [12–14,20,21] and the possible activity of DME hydrolysis to methanol [16], and it shows maximum temperature on CZA–ZrFER(0). The proper acidity on CZA–ZrFER(1) and CZA–ZrFER(3) with low desorption temperature of T_d2 helps suppress the byproduct formation such as hydrocarbons and CO_2. The two desorption peaks (T_d1 and T_d2) in Fig. 2 are integrated and their sum is used to calculate the acidic sites quantitatively. The values are shown in Table 3. The acidic site of Zr-modified ferrierite before the addition of CZA components shows an amount of acidic sites around 1.375–1.490 mmol NH_3/g as a function of Zr content and the acidic sites are maximum on the 3 wt.% Zr-modified ferrierite. This implies that the Zr modification of ferrierite surface up to 3 wt.% could enhance the amount of acidic sites slightly due to the well dispersion of Zr precursor on ferrierite surface. At higher Zr content of around 5 wt.%, the acid sites decrease due to the aggregation of Zr component at the outer surface of ferrierite as confirmed by the variation of ferrierite mesopore structure in Fig. 1. With these findings, Zr modification of ferrierite, before the addition of CZA component, could also alter the dispersion of CZA component and its reducibility by changing the acidity of ferrierite.

In order to understand the variation of acidity on CZA–ZrFER catalysts as a function of Zr content, NH_3-TPD was carried out on all CZA–ZrFER bifunctional catalysts. The total acidic sites ($T_d1 + T_d2$)

Table 3
Acidity of fresh CZA–ZrFER bifunctional catalysts by NH_3-TPD.

Catalyst	Acidic sites (mmol NH_3/g)			T_{max} of T_d2 (°C)	Acidic sites (mmol NH_3/g)[a]
	T_d1	T_d2	Total ($T_d1 + T_d2$)		
CZA–ZrFER(0)	0.211	1.126	1.337	291	1.457
CZA–ZrFER(1)	0.223	1.090	1.313	277	1.486
CZA–ZrFER(3)	0.209	0.959	1.168	275	1.490
CZA–ZrFER(5)	0.258	0.782	1.040	280	1.375

[a] The acidic sites of the Zr-modified ferrierite before the addition of CZA components.

steadily decreases to the value of 1.040 on CZA–ZrFER(5) from 1.337 on CZA–ZrFER(0) with the same trend in acidic sites of T_d2. Interestingly, the number of acidic sites of T_d1 is minimized on CZA–ZrFER(3) around 0.209 mmol NH_3/g catalyst which is showing high catalytic performance. The presence of a strong acidic site and its abundance is not beneficial for methanol dehydration due to the possibility of enhancing byproduct formation and hydrolysis of DME to methanol [12–14,16,20,21]. In general, the abundance of acid sites on the Zr-modified ferrierite (3 wt.% Zr on ferrierite) is possibly a manifestation of the high dispersion of CZA component during the coprecipitation of CZA component in the slurry of ZrFER (coprecipitation–impregnation method) and it further alters the amount of acid sites of CZA–ZrFER bifunctional catalyst by blocking the surface acid sites of ferrierite as mentioned by Flores and da Silva [22]. The large amount of acidic sites on ferrierite with 3 wt.% Zr modification and low total amount of acidic site of T_d1 on CZA–ZrFER(3) substantiate these phenomena on our samples as well. In addition, the hydrolysis of DME to methanol could occur on strong acidic site under the present reaction conditions and its activity increase with the increase of acidic strength of zeolites [16]. The DME selectivity on the CZA–ZrFER bifunctional catalyst is related with the amount of acidic sites of T_d1. With the increase of T_d1 sites corresponding to the acid sites contributed by the zeolite matrix alone [20] and an acidic strength of T_d2, the hydrolysis of DME is much favorable and eventually results in showing low selectivity to DME, especially on the bifunctional CZA–ZrFER(0) catalyst. Therefore, the CZA–ZrFER(3) catalyst possessing moderate amount of acidic site ($T_d1 + T_d2$) with a small amount of strong acidic site (low desorption temperature of T_d2) shows the highest CO conversion and DME selectivity.

In addition to the amount of acidic sites and their acidic strength, the reducibility of copper oxide is also an important variable to obtain a high catalytic activity on bifunctional catalysts. The high concentration of methanol formed could be responsible for the high selectivity to DME in the consecutive reaction on bifunctional catalyst due to the lowest activation barrier for the adsorption pathway of two contiguous methanol molecules [19]. Furthermore, the Zr modification with different loadings on ferrierite zeolite also influences the dispersion of CZA component and their reducibility by changing the acidity of Zr-modified ferrierite. This was further confirmed by conducting TPR experiments as shown in Fig. 3 and N_2O titration method to measure the metallic surface area and particle size of fresh bifunctional catalysts as summarized in Table 4. All CZA–ZrFER catalysts were easily reduced below 300 °C with a single stage reduction during the pretreatment with H_2 at 250 °C for 4 h before activity test except for the CZA–ZrFER(0). The satellite peak at 317 °C on CZA–ZrFER(0) suggests the heterogeneous distribution of CZA component with strong interaction with ferrierite zeolite. With the increase of Zr content up to 3 wt.% in CZA–ZrFER catalyst, the maximum of the reduction peak is shifted to lower temperature

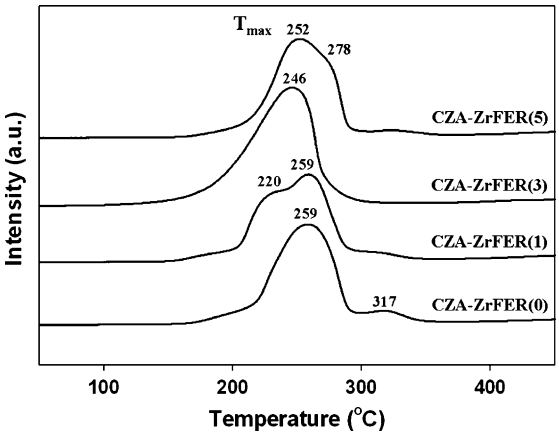

Fig. 3. TPR profiles on the bifunctional CZA–ZrFER catalysts.

from 259 to 246 °C. However, it increases 252 °C with a shoulder peak at around 278 °C when the ferrierite was modified with 5 wt.% Zr. Interestingly, the two maxima were observed at 220 and 259 °C on the CZA–ZrFER(1) catalyst and this observation also suggests a heterogeneous distribution of CZA component on Zr-modified ferrierite. The formation of homogeneous microstructure with a similar chemical composition plays an important role to obtain a high catalytic activity in Cu/ZnO system [23]. The homogeneous distribution of active component like copper could be explained by considering the reduction patterns of TPR peaks. As shown in Fig. 3, CZA–ZrFER(3) reveals one sharp reduction peak at the maximum temperature of 246 °C and the others show one reduction peak with a shoulder peak above 250 °C. The presence of shoulder peaks at high temperature with main reduction peak represents the non-homogeneous distribution of copper species in CZA component, especially for CZA–ZrFER(1) and CZA–ZrFER(5). This homogeneous distribution of copper species in CZA component is responsible for the suppressed sintering and possible redispersion of copper microstructures. The lower reduction temperature of 246 °C observed on CZA–ZrFER(3) catalyst is also accompanied by an appropriate acidic strength as obtained by NH_3-TPD analysis. Although Zr modification of ferrierite before the addition of CZA component did not significantly influence the acidic properties of ferrierite (Fig. 2 and Table 3), its modification by the addition of proper amount of 3 wt.% Zr changes the dispersion and reducibility of CZA component on bifunctional CZA–ZrFER catalysts due to the variation of acidity attributed to the different distribution of Zr on the ferrierite surface, and eventually alters the acidic properties of the finished bifunctional catalysts by the extent of blockage of acid sites with CZA component [22]. Therefore, it is proposed that Zr modification on acidic site on bare ferrierite in the case of the above discussed catalysts could change

Table 4
Copper surface area and particle size on CZA–ZrFER bifunctional catalysts by using the N_2O titration method, XRD and XPS.

Catalyst	N_2O titration			XRD		XPS	TOF[d]
	Surface area of copper (m^2/g)		Metallic copper particle size (nm)[a]	Particle size of CuO (nm)[b]		I_{Cu}/I_{Al}[c]	
	Before reaction	After reaction		Before reaction	After reaction		
CZA–ZrFER(0)	3.49	0.90	64.2	11.5	12.5	15.86	9.70
CZA–ZrFER(1)	3.11	1.80	72.0	11.4	13.8	8.36	5.82
CZA–ZrFER(3)	3.90	4.23	57.4	11.8	11.9	6.45	3.83
CZA–ZrFER(5)	1.54	0.72	145.4	12.3	13.9	10.55	11.84

[a] The particle size of Cu before reaction was calculated by using the equation of 6000/(8.92 × Cu metal surface area/Cu fraction in gram catalyst).
[b] The average particle size of CuO before and after reaction was calculated from the value of full width at half maximum (FWHM) at $2\theta = 38.6°$.
[c] The experimental electron intensity ratio for Cu and Al (I_{Cu}/I_{Al}) was obtained by XPS analysis on the used bifunctional catalysts.
[d] TOF (s^{-1}) was calculated by using the rate constant derived from CO conversion and copper surface area after reaction.

the acidity depending on the extent of homogeneously distributed Zr species and eventually resulting in changing the dispersion of CZA component and reducibility.

As shown in Table 4, the particle size of reduced metallic copper was calculated by using the equation of 6000/(8.92 × Cu metal surface area/Cu fraction in gram catalyst) [15]. From the results of N_2O titration, the metallic copper surface area is in the range of 1.54–3.90 m^2/g and the calculated particle size of metallic copper (Dp) is in the range of 57.4–145.4 nm. On CZA–ZrFER(3) shows larger surface area of 3.90 m^2/g and smaller particle size of 57.4 nm compared to that of the others. The variation of copper particle size on the fresh bifunctional CZA–ZrFER catalysts is well correlated with the variation of acidity of Zr-modified ferrierite. With the increase of acidity of Zr-modified ferrierite, the dispersion of CZA component increases resulting in higher metallic surface area and smaller particle size of copper. The facile reducibility of copper oxides with high surface area of metallic copper and moderate acidic strength of CZA–ZrFER catalysts is responsible for the observed high CO conversion and selectivity to DME on CZA–ZrFER(3).

3.3. Correlation between catalytic activity and active sites at steady state

The variation of catalytic activity during 18 h of evaluation, as shown in Fig. 4, reveals that the deactivation of CZA–ZrFER catalyst with Zr modification is very low and it is stabilized at the very beginning of reaction time. By controlling strong acidic sites on zeolite by addition of basic metal components, the catalyst stability could be enhanced due to the suppression of carbon deposition [20]. The unmodified CZA–ZrFER(0) catalyst only shows a steady decrease in activity from around 34% to 30% for 18 h on stream. The CZA component for synthesis of methanol has been widely investigated by the addition and variation of Zr component to enhance the copper dispersion and reducibility which in turn resulted in the enhancement of catalytic activity [24,25]. The introduction of Zr-modified ferrierite during the preparation of bifunctional Cu–ZnO–Al_2O_3/ZrFER catalyst in the present investigation also showed positive effects with respect to catalyst stability and DME selectivity.

To further understand the variation in catalytic activity of CZA–ZrFER, the used catalysts were characterized by XRD analysis, copper surface area measurement by N_2O titration method, XPS, TEM and DRIFT analyses. As shown in Fig. 5, X-ray diffraction patterns of the fresh and used bifunctional catalysts reveal the structural integrity of ferrierite (particularly with the appearance of peaks below $2\theta = 30^\circ$) in all samples without detection of Zr oxide suggesting a good dispersion with small size particles. The two distinct peaks at $2\theta = 35.6^\circ$ and 38.6° represent the well-dispersed CuO species and the broad peak at $2\theta = 43.3^\circ$ is due to metallic copper. The intensity of peaks related to CuO and metallic Cu slightly increased on CZA–ZrFER(5), suggesting the formation of larger CZA particles, compared to that on CZA–ZrFER(1) and CZA–ZrFER(3). The variation of average particle size of CuO is not significantly altered according to the kind of CZA–ZrFER catalysts and it is found to be in the range of 11.4–12.3 nm for the fresh bifunctional catalysts as shown in Fig. 5(A) and Table 4. Furthermore, the difference in average particle size of CuO between fresh and used catalysts (Fig. 5(B)) is smaller on CZA–ZrFER(3) which is suggesting suppression of sintering phenomena during the STD reaction. The average particle size of copper calculated by using the intense XRD peaks from FWHM values is not suited with the present investigation due to the coexistence of CuO and metallic Cu for the used bifunctional catalysts and its nature of uneven size distribution, therefore, additional characterization to measure copper surface area and particle size in the reduced state by N_2O titration method was adopted. On the fresh CZA–ZrFER catalysts, metallic copper surface area was found to be around 3.90 m^2/g which revealed smaller particle size of 57.4 nm in the CZA–ZrFER(3) sample as shown in Table 4. However, at high Zr content on CZA–ZrFER(5), the copper surface area was reduced larger to 1.54 m^2/g leading to particle size of 145.4 nm. The dispersion of CZA component is much higher on 3 wt.% Zr-modified ferrierite due to the enhanced amount of surface acid sites resulting in the increased number of sites to be impregnated with the precipitated CZA components. Since the characterization of used CZA–ZrFER catalyst might be more representative to correlate

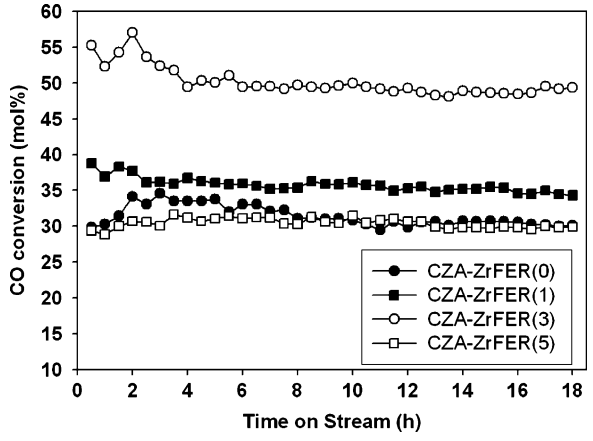

Fig. 4. CO conversion with time on stream on the bifunctional CZA–ZrFER catalysts.

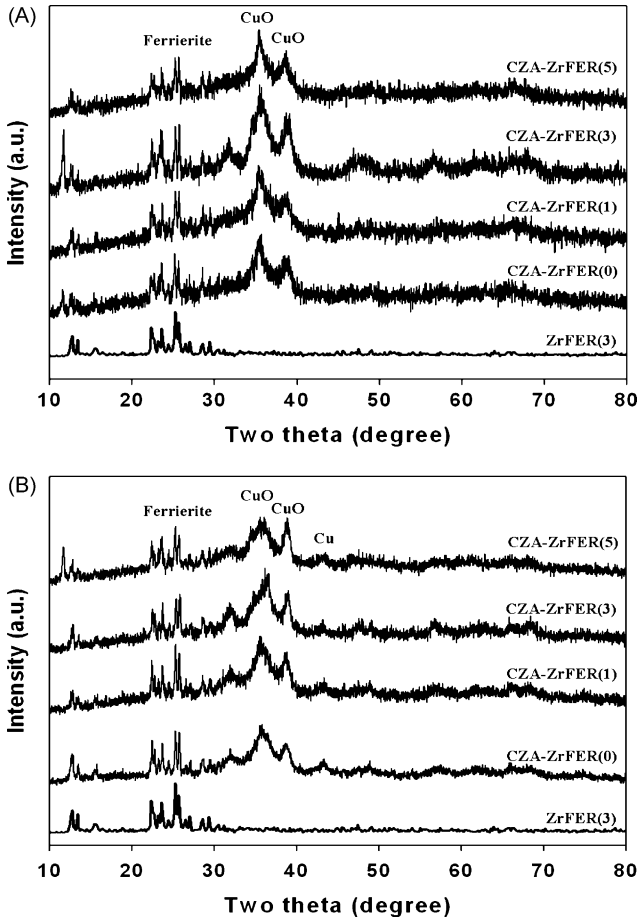

Fig. 5. XRD patterns of the (A) fresh and (B) used bifunctional CZA–ZrFER catalysts.

with the real catalytic phenomena, these used bifunctional catalysts were characterized to measure the copper surface area and particle size after reduction at 250 °C and the results are shown in Table 4. The results indicate that the copper surface area and particle size correlate well with the steady-state catalytic activity. Due to high surface area and smaller particle size (4.23 m^2/g and 53.0 nm, respectively), CZA–ZrFER(3) showed high catalytic activity in terms of CO conversion and DME selectivity. Severe sintering of copper species on CZA–ZrFER(0) and CZA–ZrFER(5) after STD reaction was observed and they eventually showed a low catalytic activity. The unmodified and 5 wt.% Zr-modified bifunctional CZA–ZrFER catalysts show low catalytic activity as they displayed a low metallic copper surface area of around 0.90 and 0.72 m^2/g and concomitant increase of copper particle size. The particle size of CuO after reaction was calculated from the value of full width at half maximum (FWHM) at $2\theta = 38.6°$. As shown in Table 4, the particle size is in the range of 11.9–13.9 nm, and that size is minimum on CZA–ZrFER(3) which is also confirmed by TEM analysis and N_2O titration in the following paragraph.

The Cu $2p_{3/2}$ and Zr $3d_{5/2}$ photoelectron spectra of the used bifunctional catalysts are shown in Fig. 6 and the binding energy (BE) of the same was corrected by adjusting with the reference BE of Al 2s (120.4 eV). The BE of Cu $2p_{3/2}$ at ~930 eV is generally assigned to Cu^+ and that ~933.5 eV to Cu^{2+} with the characteristic satellite peaks between 940 and 945 eV due to the electron shake-up process. The BE of Zr $3d_{5/2}$ peak at ~182 eV indicates that Zr species is present as ZrO_2 [8,26,27]. Furthermore, the shift in BE of Cu $2p_{3/2}$ to lower value and the suppression of satellite peak intensity are mainly attributed to the presence of Cu^+ and/or Cu^0 phase on the catalyst surface. The state of ZnO is mainly in the form of oxygen-deficient phase such as $(Zn^{(2-\delta)+}, 0 < \delta < 2)$ [8]. In addition, the synergistic effect on methanol synthesis could be obtained by the co-presence of two-dimensional Cu^0–Cu^+ layer which causes a strong molecular instead of dissociative adsorption of CO (not active for methanol synthesis) through electron back-donation from metal to CO $2\pi^*$. Its synergistic effect is further enhanced by the presence of $Zn^{(2-\delta)+}$ due to the stabilization of Cu^+ [27,28]. All our bifunctional CZA–ZrFER catalysts showed a distinctive BE of Cu $2p_{3/2}$ around 930 eV and it suggests the co-presence of Cu^0–Cu^+ layer. The shift to lower BE of Cu $2p_{3/2}$ on CZA–ZrFER(3) compared to CZA–ZrFER(0) and CZA–ZrFER(5) further suggests a well-dispersed two-dimensional Cu^0–Cu^+ layer which is active for methanol synthesis and this is also confirmed by N_2O titration and XRD analysis. In addition to the BE investigation, the experimental electron intensity ratio for Cu and Al (I_{Cu}/I_{Al}) could also correlated with copper particle size which was well established by many researchers in the filed of cobalt-based catalysts [29]. With the increase of I_{Cu}/I_{Al} ratio, the particle size of copper decreases with the assumption of monolayer coverage of copper species. Although the calculated particle size from XPS peak intensity ratio is not well matched due to the presence of agglomerated particles with heterogeneous distribution, the I_{Cu}/I_{Al} values do give some clues for estimation of copper particle size. The ratio of I_{Cu}/I_{Al} values, shown in Fig. 6 (Cu $2p_{3/2}$ and Al 2s) and Table 4 on our samples, are 15.86, 8.36, 6.45 and 10.55 for CZA–ZrFER(0), CZA–ZrFER(1), CZA–ZrFER(3) and CZA–ZrFER(5), respectively. The lower value of I_{Cu}/I_{Al} for CZA–ZrFER(3) suggests small copper particle size formation with well-dispersed two-dimensional Cu^0–Cu^+ layer and low BE because of highly exposed Zr-modified ferrierite surface. It is believed that good dispersion of copper species with the presence of partially reduced Zn on CZA–ZrFER(3) is responsible for the high methanol synthesis activity, coupled with the acidity of Zr-modified ferrierite.

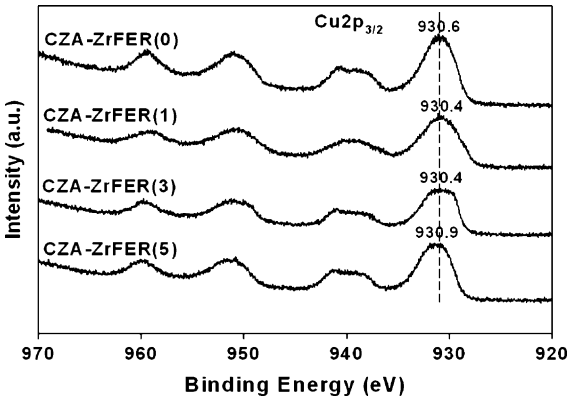

Fig. 6. XPS analysis of the used bifunctional CZA–ZrFER catalysts.

To confirm the results of N_2O titration method and XPS analysis (I_{Cu}/I_{Al} ratio), the particle size of fresh and used catalysts after 18 h was further determined by TEM analyses. Fig. 7 shows the particle sizes of CZA components and their morphology. All bifunctional catalysts show agglomerated sphere-type granules of CZA with multimodal particle distribution, with the size ranging between 10 and 100 nm which is distributed on the Zr-modified ferrierite. In order to provide evidence for sintering of CZA component, the particle sizes of fresh and used CZA–ZrFER(0) catalysts are represented (Fig. 7(A-1) and (A-2)) and CZA–ZrFER(3) catalyst (Fig. 7(B-1) and (B-2)). The particle size of the used CZA–ZrFER(3) catalyst is not much altered compared to that of fresh one, however, the sintering on CZA–ZrFER(0) after reaction was observed significantly which is also consistent with the results of N_2O titration. The CZA particles on CZA–ZrFER(3) after reaction are much smaller than CZA–ZrFER(0) and the trend of particle size variation is similar with the results of N_2O titration, XRD and XPS analyses. These small CZA particles on 3 wt.% Zr-modified ferrierite are attributed to the high catalytic activity due to facile reducibility with a homogeneous distribution of CZA component with their proper electronic states confirmed by TPR, N_2O titration, XPS and TEM images. In addition, TEM-EDX analysis also shows that the sphere-type particles are attributed to CZA component on Zr-modified ferrierite. The homogeneous distribution of copper in CZA granules is probably responsible for the suppressed sintering and redispersion of copper microstructure, especially on CZA–ZrFER(3). Thus, even after undergoing considerable change in the catalyst functionality, CZA–ZrFER(3) emerges as the best among four catalysts.

The DRIFT spectra of adsorbed CO on the used CZA–ZrFER catalysts are shown in Fig. 8. The absorbance band around 2110 cm^{-1} could be assigned to the adsorbed CO molecule at Cu^0 and 2154 cm^{-1} for Cu^+ [30]. The high electron density on the reduced copper species could increase the availability of electrons in the d-orbital by electron back-donation from metal particle to the adsorbed CO molecule and eventually reduce the C–O bonding energy thus shifting it to lower CO frequency. In our bifunctional CZA–ZrFER catalysts, the frequency of adsorbed CO shifted to lower value with the increase of Zr content up to 3 wt.% from 2114 to 2110 cm^{-1} and increased again to 2110 cm^{-1} on CZA–ZrFER(5). The lower frequency of adsorbed CO on CZA–ZrFER(3) suggests the facile activation of CO with low activation energy. Interestingly, CZA–ZrFER(3) catalyst revealed the abundant Cu^+ sites compared to others which is assigned to the adsorbed CO molecule at the frequency of 2154 cm^{-1} as shown in Fig. 8. In general, the high activity on methanol synthesis could be assigned to the co-presence of two-dimensional Cu^0–Cu^+ layer with a strong adsorption of CO on copper surface [27,28]. Therefore, the low activation energy of CO (low frequency of adsorbed CO) and co-presence of Cu^0–Cu^+ species is mainly responsible for showing a high activity on the bifunctional CZA–ZrFER(3) catalyst.

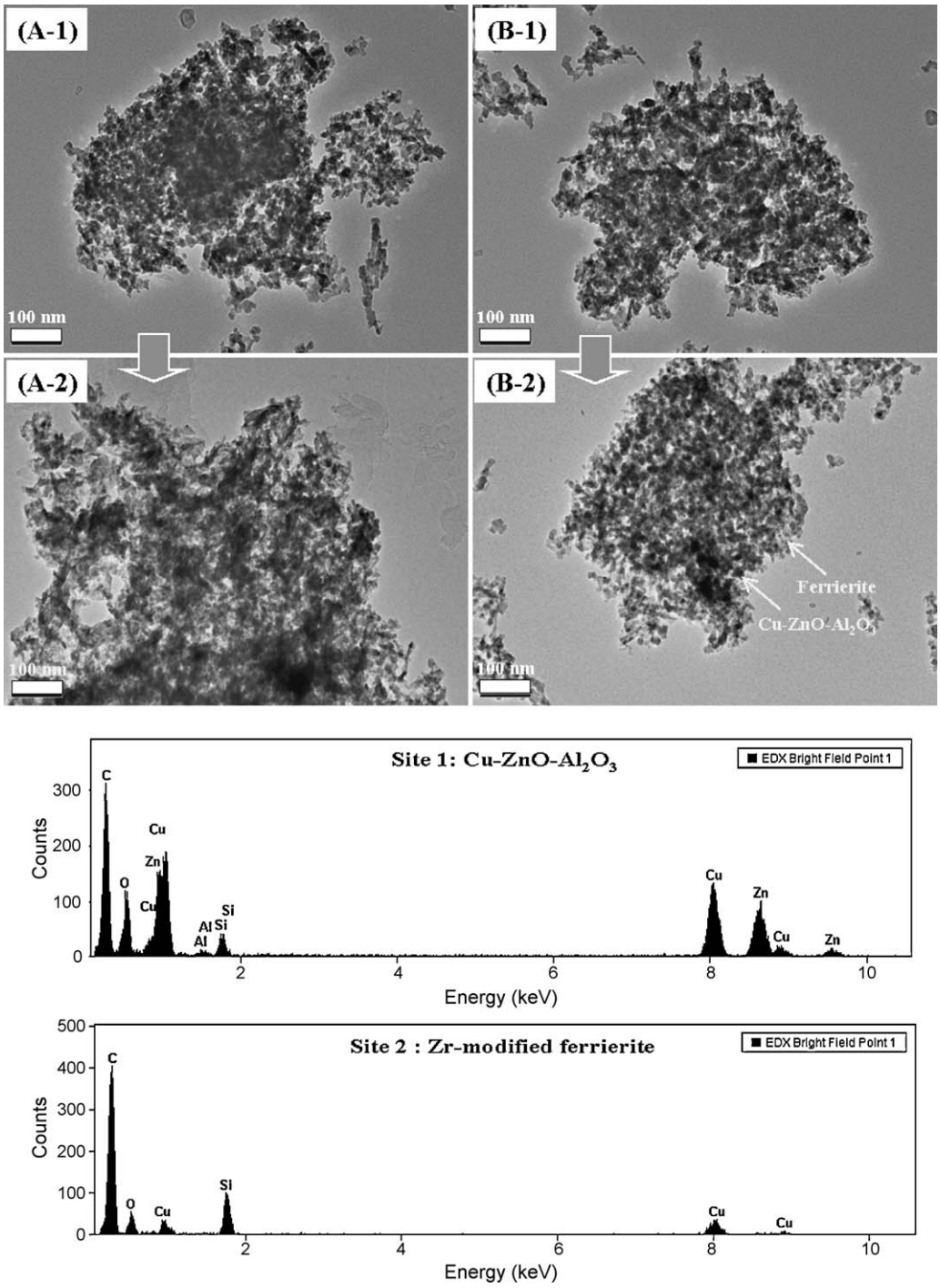

Fig. 7. TEM analysis of the fresh and used bifunctional CZA–ZrFER catalysts. (A-1) Fresh CZA–ZrFER(0); (A-2) used CZA–ZrFER(0); (B-1) fresh CZA–ZrFER(3); (B-2) used CZA–ZrFER(3).

Interestingly, the turnover frequency (TOF; s^{-1}) values on CZA–ZrFER bifunctional catalysts (calculated by using the copper surface area after reaction for 18 h and rate constant derived from CO conversion) showed a minimum value of 2.79 on CZA–ZrFER(3) which showed highest CO conversion. The TOF values are inversely correlated with the CO conversion which suggests that STD (syngas to DME) reaction on the bifunctional CZA–ZrFER catalyst is a kind of structure-sensitive reaction. The CO conversion and TOF were displayed against metallic copper surface area of used catalysts and the result is shown in Fig. 9. The CO conversion correlated linearly with the copper surface area which means that a high surface area of metallic copper is beneficial to obtain a high catalytic activity. However, the TOF values on bifunctional CZA–ZrFER catalysts show parabolic decrease versus the increase of copper surface area (inversely decrease of copper particle size). The CZA–ZrFER(3) catalyst showed a high CO conversion due to the higher metallic copper surface area of 4.23 m^2/g and smaller particle size of 53.0 nm reveals a lower TOF value of 2.79 and vice versa in the case of CZA–ZrFER(5) catalyst. As reported by Blaszkowski and van Santen [19], the partial pressure of previously formed methanol could enhance the DME selectivity due to the lowest activation barrier for the pathway involving two methanol molecules adsorption concomitantly in a direct DME synthesis from syngas by a consecutive reaction. Furthermore, the existence

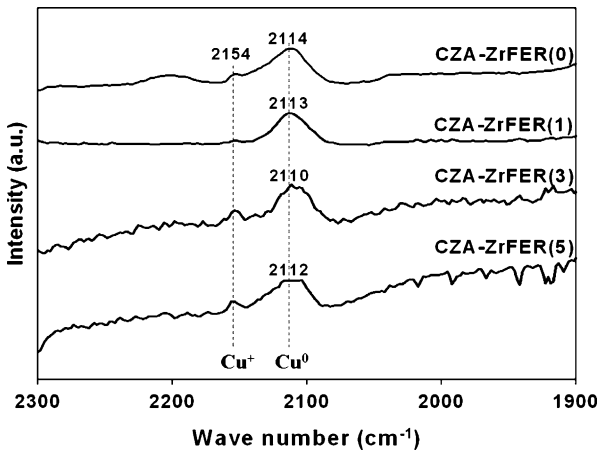

Fig. 8. DRIFT spectra of the used CZA–ZrFER catalysts.

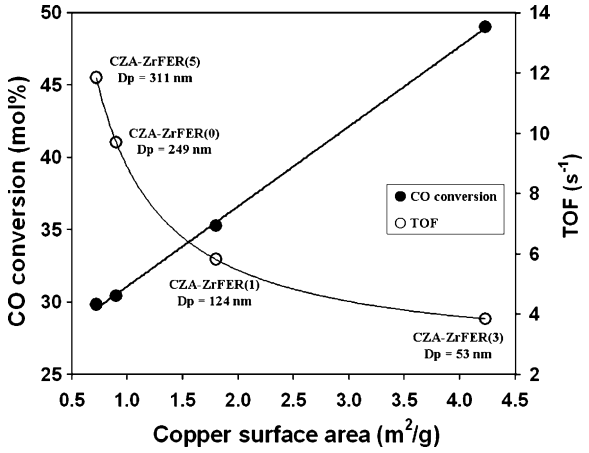

Fig. 9. Correlation of CO conversion and TOF value with respect to copper surface area on the bifunctional CZA–ZrFER catalysts.

of larger CZA particles on the outer surface of Zr-modified ferrierite on CZA–ZrFER(5) with an uneven distribution of Zr species is responsible for the presence of strong acidic sites in mesopore of ferrierite even after precipitation of CZA component. These sites are not suitable sites to obtain high DME selectivity and CO conversion due to the low surface area of metallic copper and strong acidic strength for the facile adsorption of two methanol molecules followed by dehydration to DME due to the possible high activity for hydrolysis of DME to methanol. With larger copper particles, the higher amount of stronger acidic sites which is revealed by high desorption temperature of T_d2 could be obtained due to the low blockage of acidic sites on Zr-modified ferrierite. Furthermore, since the intrinsic rate for methanol synthesis for syngas is much lower than that of methanol dehydration to DME [10,14], the high concentration of methanol formed on the active copper surfaces, e.g. on CZA–ZrFER(3) shows that high metallic copper surface area is responsible for the high DME selectivity. Therefore, the high production rate of DME on the bifunctional CZA–ZrFER(3) catalyst is mainly attributed to the high production rate of methanol with a high metallic copper surface area and moderate amount of acidic sites (T_d1 and T_d2) with low desorption temperature of T_d2, however, its intrinsic rate is suppressed by the reduced number of adjacent acid sites for two methanol molecules adsorption on CZA–ZrFER(3) which is suppressed by the deposition of small CZA components. Additionally, the extra hydrogen produced by water–gas-shift reaction accelerates the conversion of CO and this is also in agreement with the observation of high CO_2 formation.

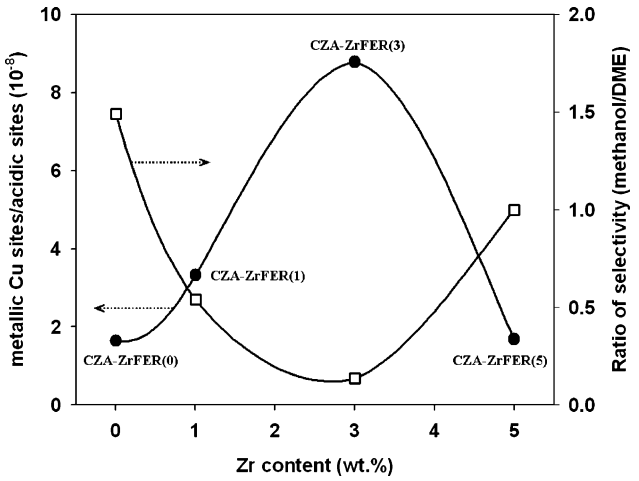

Fig. 10. Effects of Zr content on the ratio of metallic copper sites to acidic sites and the ratio of selectivity (methanol/DME).

To summarize the effects of Zr concentration on ferrierite, the ratio of metallic copper sites to acidic sites and the ratio of selectivity (methanol/DME) with respect to Zr concentration are represented in Fig. 10. At the optimum concentration of Zr of 3 wt.%, the lower ratio of methanol/DME selectivity and higher ratio of metallic copper site/acidic sites ($T_d1 + T_d2$) was observed. This suggests that the generated methanol molecules are converted to DME much faster and easily. Therefore, by considering TOF values in Fig. 9, it also suggests that the rate determining reaction is methanol synthesis instead of methanol dehydration on CZA–ZrFER bifunctional catalyst. The observed low TOF value on CZA–ZrFER(3) is mainly attributed to low concentration of adjacent acid sites for methanol dehydration even though it shows a high metallic surface area of copper with facile reducibility. However, the high CO conversion on CZA–ZrFER(3) can be obtained due to the fast reaction of methanol dehydration which is helping to produce extra hydrogen by WGS reaction and consequently enhancing the activity of CO hydrogenation to methanol. In addition, the high TOF values with low DME selectivity and CO conversion observed on CZA–ZrFER(0) and CZA–ZrFER(5) is possibly attributed to the activity for the hydrolysis of DME to methanol on the strong acidic sites and a low surface area of copper which is also responsible for the low concentration of methanol on the surface of bifunctional catalyst. Thus, CZA–ZrFER bifunctional catalysts, Zr modification of ferrierite moderate the acidic site properties by reducing the strong acidic sites and with concomitant enhancement of the dispersion of CZA components on CZA–ZrFER(3) with high reducibility with a small particle size and proper electronic state of metallic copper species results in the enhancement of CO conversion and DME selectivity.

4. Conclusions

The CZA–ZrFER bifunctional catalysts with 3 wt.% Zr showed stable activity in the direct synthesis of DME from H_2-deficient and biomass-derived syngas. The high catalytic performance on CZA–ZrFER(3) bifunctional catalyst compared to the other catalysts is mainly attributed to the facile reducibility of copper species with the possible co-presence of Cu^+–Cu^0 species with high metallic surface area and moderate amount of acidic sites and their weak strength by enhancing the homogeneous distribution of copper species in Cu–ZnO–Al_2O_3 component after Zr modification of ferrierite which eventually resulted in the proper CO hydrogenation activity and acidic function for dehydration of methanol. The

abundance of methanol on the surface of the catalyst also enhances the DME selectivity on the CZA–ZrFER(3) catalyst and the concomitant formation of extra hydrogen by WGS accelerated the CO hydrogenation. In addition, the highly dispersed small Cu–ZnO–Al_2O_3 component on CZA–ZrFER(3) catalyst could suppress the strong acidic sites on Zr-modified ferrierite and eventually enhance the DME selectivity with a low byproduct formation. Furthermore, in the present investigation, it is observed that low intrinsic rate (TOF) on CZA–ZrFER(3), even though it shows high CO conversion, is mainly attributed to the high blockage of acidic sites of Zr-modified ferrierite by the formation of smaller Cu–ZnO–Al_2O_3 component and the suppression of adjacent acid sites for adsorbing two methanol molecules concomitantly.

References

[1] (a) T.A. Semelsberger, R.L. Borup, H.L. Greene, J. Power Sources 156 (2006) 497–511;
(b) G. Cai, Z. Liu, R. Shi, C. He, L. Yang, C. Sun, Y. Chang, Appl. Catal. A 125 (1995) 29–38.
[2] (a) M. Ruggiero, G. Manfrida, Renewable Energy 16 (1999) 1106;
(b) M. Nilsson, K. Jansson, P. Jozsa, L.J. Pettersson, Appl. Catal. B 86 (2009) 18;
(c) K. Faungnawakij, Y. Tanaka, N. Shimoda, T. Fukunaga, R. Kikuchi, K. Eguchi, Appl. Catal. B 74 (2007) 144.
[3] S.D. Kim, S.C. Baek, Y.H. Lee, K.W. Jun, M.J. Kim, I.S. Yoo, Appl. Catal. A 309 (2006) 139–143.
[4] L. Wang, Y. Qi, Y. Wei, D. Fang, S. Meng, Z. Liu, Catal. Lett. 106 (2006) 61–66.
[5] (a) G.X. Jia, H.B. Ma, Y.S. Tan, Y.Z. Han, Ind. Eng. Chem. Res. 44 (2005) 2011–2015;
(b) S. Lee, A. Sardesai, Top. Catal. 32 (2005) 197–207.
[6] M. Ruggiew, G. Manfrida, Renewable Energy 16 (1999) 1106–1109.
[7] J.H. Fei, M.X. Yang, Z.Y. Hou, X.M. Zheng, Energy Fuels 18 (2004) 1584–1587.
[8] K. Sun, W. Lu, F. Qiu, S. Liu, X. Xu, Appl. Catal. A 252 (2003) 243–249.
[9] J. Xia, D. Mao, B. Zhang, Q. Chen, Y. Tang, Catal. Lett. 98 (2004) 235–240.
[10] D. Mao, W. Yang, J. Xia, B. Zhang, Q. Song, Q. Chen, J. Catal. 230 (2005) 140–149.
[11] T. Takeguchi, K.I. Yanagisawa, T. Inui, M. Inoue, Appl. Catal. A 192 (2000) 201–209.
[12] S.H. Kang, J.W. Bae, K.W. Jun, H.S. Potdar, Catal. Commun. 9 (10) (2008) 2035–2039.
[13] P.S. Sai Prasad, J.W. Bae, S.H. Kang, Y.J. Lee, K.W. Jun, Fuel Process. Tech. 89 (2008) 1281–1286.
[14] J.W. Bae, H.S. Potdar, S.H. Kang, K.W. Jun, Energy Fuels 22 (1) (2008) 223–230.
[15] J.W. Evans, M.S. Wainwright, A.J. Bridgewater, D.J. Yong, Appl. Catal. 7 (1983) 75–83.
[16] T.A. Semelsberger, K.C. Ott, R.L. Borup, H.L. Greene, Appl. Catal. B 61 (2005) 281.
[17] K.L. Ng, D. Chadwick, B.A. Toseland, Chem. Eng. Sci. 54 (1999) 3587–3592.
[18] G. Jia, Y. Tan, Y. Han, Ind. Eng. Chem. Res. 45 (2006) 1152–1159.
[19] S.R. Blaszkowski, R.A. van Santen, J. Phys. Chem. B 101 (1997) 2292–2305.
[20] D. Jin, B. Zhu, Z. Hou, J. Fei, H. Lou, X. Zheng, Fuel 86 (2007) 2707–2713.
[21] Y. Fu, T. Hong, J. Chen, A. Auroux, J. Shen, Thermochim. Acta 434 (2005) 22–26.
[22] J.H. Flores, M.I.P. da Silva, Colloid Surf. A 322 (2008) 113–123.
[23] B.L. Kniep, F. Girgsdies, T. Ressler, J. Catal. 236 (2005) 34.
[24] C. Yang, Z. Ma, N. Zhao, W. Wei, T. Hu, Y. Sun, Catal. Today 115 (2006) 222–227.
[25] J. Sloczynski, R. Grabowski, P. Olszewski, A. Kozlowska, J. Stoch, M. Lachowska, J. Skrzypek, Appl. Catal. A 310 (2006) 127–137.
[26] G.X. Qi, X.M. Zheng, J.H. Fei, Z.Y. Hou, J. Mol. Catal. A 176 (2001) 195–203.
[27] Y. Okamoto, K. Fukino, T. Imanaka, S. Teranishi, J. Phys. Chem. 87 (1983) 3740–3747.
[28] J. Nakamura, T. Uchijima, Y. Kanai, T. Fujitani, Catal. Today 28 (1996) 223–230.
[29] (a) A.Y. Khodakov, A. Griboval-Constant, R. Bechara, V.L. Zholobenko, J. Catal. 206 (2002) 230–241;
(b) F.P.J.M. Kerkhof, J.A. Moulijn, J. Phys. Chem. 83 (1979) 1612–1619.
[30] H.Y. Chen, L. Chen, J. Lin, K.L. Tan, Inorg. Chem. 36 (1997) 1417–1423.